

Compressible Mixing Layer: Linear Theory and Direct Simulation

N. D. Sandham* and W. C. Reynolds†
Stanford University, Stanford, California

Results from linear stability analysis are presented for a wide variety of mixing layers, including low-speed layers with variable density and high Mach number mixing layers. The linear amplification predicts correctly the experimentally observed trends in growth rate that are due to velocity ratio, density ratio, and Mach number, provided that the spatial theory is used and the mean flow is a computed solution of the compressible boundary-layer equations. It is found that three-dimensional modes are dominant in the high-speed mixing layer above a convective Mach number of 0.6, and a simple relationship is proposed that approximately describes the orientation of these waves. Direct numerical simulations of the compressible Navier-Stokes equations are used to show the reduced growth rate that is due to increasing Mach number. From consideration of the compressible vorticity equation, it is found that the dominant physics controlling the nonlinear roll-up of vortices in the high-speed mixing layer is contained in an elementary form in the linear eigenfunctions. It is concluded that the linear theory can be very useful for investigating the physics of free shear layers and predicting the growth rate of the developed plane mixing layer.

Introduction

THE plane mixing layer shows a strong reduction in growth rate as Mach number is increased. Brown and Roshko¹ showed that density effects alone were not able to explain this phenomenon, which must therefore be due to compressibility. This reduction in growth rate has important implications for mixing and reaction in supersonic combustors, where the limiting process may be the time taken to mix fuel and oxidizer. The existing experimental data have been collated by Papamoschou and Roshko,² who introduced the convective Mach number as a parameter that seemed to collapse the available growth rate data. The same measure was proposed by Bogdanoff³ as a way to present the data. For the plane mixing layer between gases with equal γ (γ = the ratio of specific heats), the convective Mach number is defined by

$$M_c = \frac{U_1 - U_c}{c_1} = \frac{U_c - U_2}{c_2} \quad (1)$$

$$U_c = \frac{U_1 c_2 + U_2 c_1}{c_1 + c_2} \quad (2)$$

where U_c is the convective velocity of the large structures, U_1 and U_2 are the freestream velocities, and c_1 and c_2 are the freestream sound speeds. The convective Mach number is based on the idea that a point exists in the flow at which the total pressures of the two streams are equal. In the incompressible mixing layer, this point is the saddle point in the braid region between two structures.

Several studies of the linear stability of compressible mixing layers have been carried out over the last 20 years,⁴⁻⁸ documenting a strong reduction in the growth rate of two-dimensional disturbances in the flow as Mach number is increased.

The valuable contributions of Gropengiesser⁴ were largely overlooked at the time. He used a solution of the compressible boundary-layer equations for the base velocity and temperature profiles, rather than simple hyperbolic tangent profiles, and observed the strong growth rate of three-dimensional disturbances at high Mach numbers. Gropengiesser also found the supersonic modes of instability for two-dimensional disturbances at high Mach number, originally found by Lessen et al.,⁵ which were subsequently rediscovered by Blumen et al.⁶

The important effects of the mean velocity profile were investigated by Monkewitz and Huerre.⁹ They found that only the amplification computed by spatial theory for the Blasius mixing-layer velocity profile showed growth rate proportional to $\lambda = (U_1 - U_2)/(U_1 + U_2)$, as found in experiments. Morkovin¹⁰ makes the point that only the results from spatial stability analysis based on a mean profile satisfying the boundary-layer equations can be compared with mixing-layer experiments. The decision as to whether spatial or temporal theory should be used depends on the nature of the instability of the flow, as characterized by Huerre and Monkewitz.¹¹ If the flow is convectively unstable, as in the experiment, then the spatial theory should be used. On the other hand, if the flow is absolutely unstable, as in time-developing mixing-layer simulations, then the temporal theory should be used. Earlier attempts to transform results from the temporal theory gave poor agreement with the experimental measurements.

Recent work by Ragab and Wu⁷ shows that, as with incompressible free shear layers, the compressible mixing layer has a basically inviscid, inflectional instability and that the effect of viscosity is only to slow down the growth of disturbances. They also found that nonparallel effects are negligible in compressible mixing layers.

The objective of this work is to assess the usefulness of linear stability theory in predicting mixing-layer growth rates; to analyze the instabilities in the flow as Mach number is increased; and to simulate numerically the nonlinear development of the two-dimensional instability in the flow.

Linear Stability Methodology

In the linear calculations presented in this paper, unless otherwise noted, the mean velocity profile is a computed solution of the compressible boundary-layer equations, the mean

Received Nov. 1, 1988; presented as Paper 89-0371 at the AIAA 27th Aerospace Sciences Meeting, Reno, NV, Jan. 8-12, 1989; revision received May 24, 1989. Copyright © 1989 American Institute of Aeronautics and Astronautics, Inc. All rights reserved.

*Research Scientist; currently, German Aerospace Research Establishment (DLR), Göttingen, Federal Republic of Germany.

†Professor, Department of Mechanical Engineering. Associate Fellow AIAA.

temperature profile is found from a Crocco-Busemann relation, assuming unity Prandtl number, and the spatial stability theory is used. The Crocco-Busemann¹² relation between temperature and mean velocity is found by twice integrating the energy relation

$$\frac{d^2 T}{du^2} = M^2 (\gamma - 1) \quad (3)$$

The compressible boundary-layer equations were solved using a shooting method, described in Sandham and Reynolds.¹³ Distances are normalized by the vorticity thickness of the reference velocity profile, and velocities by the freestream velocity U_1 .

The linearized equations are obtained by using the following decomposition in the compressible Euler equations:

$$\begin{aligned} u &= \bar{u} + u', \quad v = v', \quad w = w', \quad T = \bar{T} + T', \\ \rho &= \bar{\rho} + \rho', \quad p = \bar{p} + p' \end{aligned} \quad (4)$$

Disturbances are assumed to have the form of traveling waves

$$(u', v', w', T', p') = (\hat{u}, \hat{v}, \hat{w}, \hat{T}, \hat{p}) \exp[i(\alpha x + \beta z - \omega t)] \quad (5)$$

where $\hat{u}, \hat{v}, \hat{w}, \hat{T}, \hat{p}$ are eigenfunctions depending only on the transverse coordinate y . Inside the complex exponential, ω is the frequency, and α and β are wave numbers in the streamwise (x) and spanwise (z) directions, respectively. In general, the angle of θ of a disturbance is given by

$$\tan \theta = \beta / \alpha_r \quad (6)$$

For spatial stability analysis, ω is real and α is complex whereas, for temporal analysis, α is real and ω is complex. Linear amplifications for the two cases are given, respectively, by $-\alpha_j$ and ω_i .

Two methods were used to obtain results: a direct method, solving the original system of five disturbance equations using a spectral representation of the disturbance eigenfunctions and a matrix eigenvalue solver; and a shooting method, solving the one nonlinear equation derived by Gropengieser.⁴ The methods are applicable to both the temporal and spatial stability problem for general plane free shear layers. For the mixing layer, any velocity and density ratios can be specified, and either a hyperbolic tangent or the boundary-layer mean profile can be used. Verification was made by checking results against published data,^{4,8,14,15} as well as against growth rates computed from direct numerical solutions. It was found that the shooting method gave the best results. The direct method showed poor convergence near the neutral points and for weakly amplified disturbances at high Mach number, presumably because of difficulty resolving the eigenfunctions for near-singular disturbances.

The basic philosophy adopted in these linear theory calculations is that the growth rate of the compressible mixing layer is directly related to the amplification of the most unstable mode from the linear theory, provided that 1) the spatial theory is used, and 2) the laminar solution of the compressible boundary-layer equations is used as the base flow, with vorticity thickness as the reference length scale.

The second criterion, proposed by Monkewitz and Heurre,⁹ may appear a little strange since the laminar solution, if it exists at all, appears only in the mixing layer after any splitter plate wake has diffused and before any instabilities have developed to change the mean flow. However, the profile shape computed from the solution of the boundary-layer equations is also the solution for the self-similar mixing layer, assuming an eddy-viscosity turbulence model, and may thus be expected to apply at any large distance downstream. A limiting feature of the analysis will be the accuracy of the eddy-viscosity model for the mean flow.

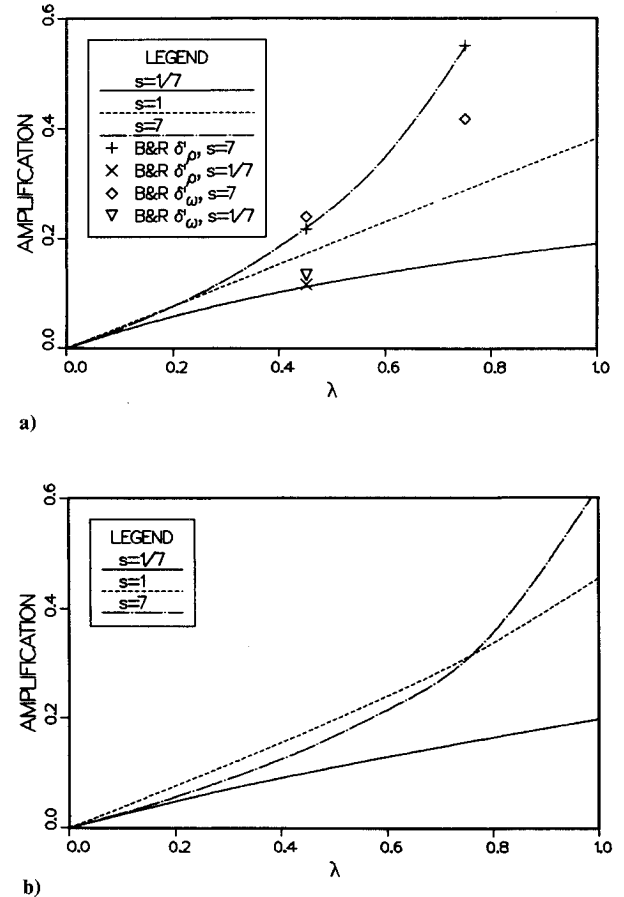


Fig. 1 Effect of velocity and density ratio on linear growth rate a) boundary-layer solution as base profile compared with experimental data from Brown and Roshko; b) hyperbolic tangent.

In the first part of the next section, this procedure is justified by consideration of flows at low Mach number, for which some experimental data exist.

Results from Linear Stability Theory

Low Mach Number Results

It was shown by Monkewitz and Huerre⁹ that, when spatial theory and the Blasius mixing-layer profile was used, the maximum amplification rate $-\alpha_j$ is proportional to $\lambda = (U_1 - U_2)/(U_1 + U_2)$. Also the best fit through the experimental data for the incompressible mixing layer with uniform density, compiled by Brown and Roshko,¹ is a straight line with growth rate $\delta' = d\delta/dx$ proportional to λ . Thus, for the incompressible mixing layer with constant density, it is already known that $|\alpha_j|_{\max}$ from linear theory is proportional to δ' from experiments. We now consider mixing layers with unequal freestream densities.

The effect of density and velocity ratio on the amplification of the most unstable wave are shown in Fig. 1a for the boundary-layer mean profile and in Fig. 1b for a hyperbolic tangent mean profile. The density ratio s is defined as ρ_2/ρ_1 , which is equal to T_1/T_2 for freestreams with equal pressures. Variation of amplification against λ is plotted for three different density ratios at Mach number 0.1 and can be compared with curves presented by Bogdanoff¹⁶ and Dimotakis.¹⁷ The agreement between the linear amplification and the experimental growth rate is good, especially when mixing-layer thicknesses based on the mean density profile are used. The ratio $-\delta'/\alpha_i$ is shown in Table 1 for the available experimental data. From these results, we conclude the following ap-

Table 1 Relationship between δ' from experiments and $|\alpha_i|_{\max}$ from linear theory

Experiment	U_2/U_1	ρ_2/ρ_1	$\delta'_\rho/ \alpha_i _{\max}$	$\delta'_\omega/ \alpha_i _{\max}$
Brown and Roshko ¹	$1/\sqrt{7}$	7	0.591	0.491
Brown and Roshko ¹	$1/\sqrt{7}$	1/7	0.623	0.537
Brown and Roshko ¹	1/7	7	0.604	0.344
Fiedler ¹⁸	0.0	1.09	0.594	—
Bogdanoff ¹⁶	0.0	0.2	0.557	—
Dimotakis and Brown ¹⁹	0.19	1.0	—	0.432

proximate relations between linear amplification and experimental growth rate:

$$\delta'_\rho \approx 0.6 |\alpha_i|_{\max} \quad (7)$$

$$\delta'_\omega \approx 0.45 |\alpha_i|_{\max} \quad (8)$$

where δ'_ρ ($= d\delta_\rho/dx$) is the growth rate measured from the mean density profile, and δ'_ω is the usual vorticity thickness growth rate. For the vorticity thickness growth rate constant, Brown and Roshko¹ proposed the best fit $\delta'_\omega = 0.181\lambda$, which would give a constant in Eq. (8) of 0.474. Their preferred expression was $\delta'_\omega = 0.162\lambda$, which would give a constant of 0.424.

Comparison of Figs. 1a and 1b shows that the linear results based on a hyperbolic tangent mean velocity profile do not show the correct trends due to density ratio.

Oblique Waves at High Mach Number

The basic effect of compressibility is first considered for the temporal stability of the time-developing mixing layer with

equal densities and temperatures, and with a simple velocity profile,

$$u = \tanh(2y) \quad (9)$$

For the equal density time-developing mixing layer, the hyperbolic tangent velocity profile is not too much in error, and we are not concerned here with experimental comparisons. The qualitative picture is exactly the same when the boundary-layer equations are solved for the mean flow, as will be seen later. Figure 2a shows the effect of increasing Mach number on amplification of two-dimensional waves. The observed trend is very similar to that found by Gropengieser⁴ for the spatial theory, including the appearance of a second mode of instability, characterized by a different phase speed $c_r = \omega_r/\alpha_r$, as evident from the plot of ω_r shown in Fig. 2b. The two-dimensional mode is strongly damped by Mach number, and only the emergence of the second mode keeps the two-dimensional mixing layer unstable at high Mach numbers. The first mode is stationary in the time-developing mixing-layer reference frame, whereas the second mode corresponds to waves traveling to the left and right. Also, we note that, in the time-developing reference frame, the Mach number of each freestream is by definition the convective Mach number.

The increasing obliquity of the most amplified waves as Mach number is increased is illustrated in Figs. 3a and 3b. In these figures, amplification is plotted against θ for various Mach numbers where, for each Mach number, the wavelength is fixed at the most amplified wavelength (including oblique waves). Figure 3a is the plot for the time-developing mixing layer from above, whereas Fig. 3b is for a spatially developing mixing layer, with $T_2/T_1 = 1.0$ and $U_2/U_1 = 0.5$ and with a compressible boundary-layer solution as the base flow. The

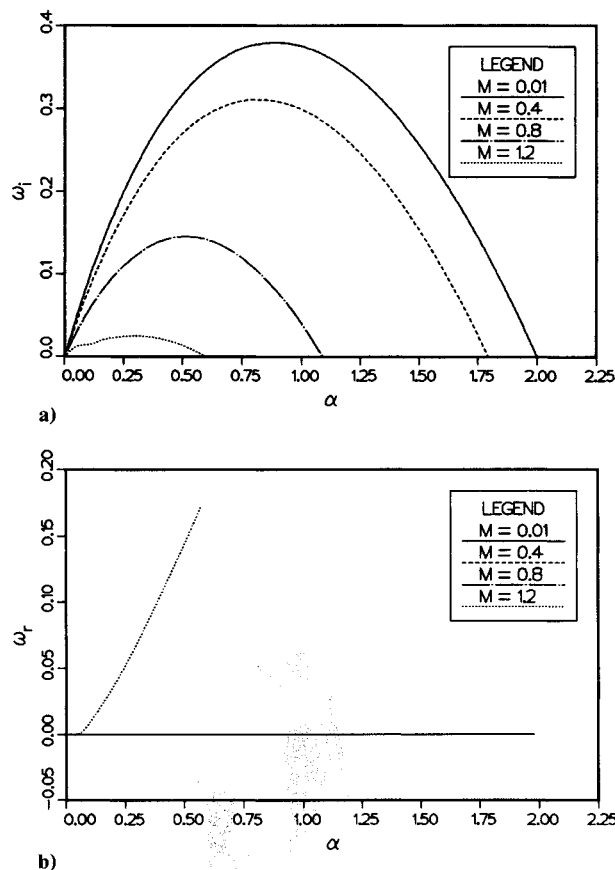


Fig. 2 Effect of Mach number on the growth of two-dimensional waves: a) ω_i ; b) ω_r .

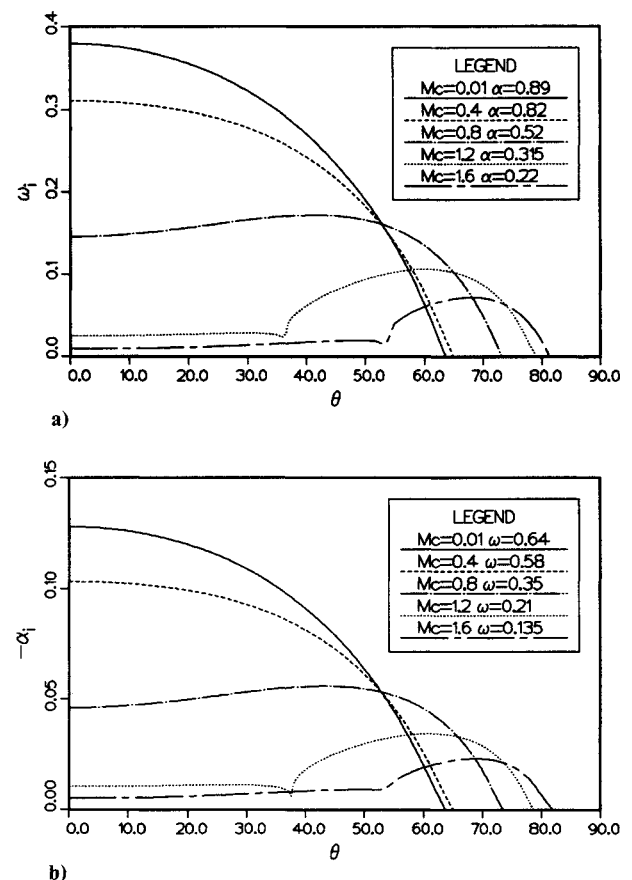


Fig. 3 Effect of obliquity on amplification: a) temporal stability with hyperbolic tangent velocity profile; b) spatial stability, with boundary-layer solution as base profile.

Table 2 Variation of $M_c \cos\theta$ for oblique waves

$T_1 = T_2, U_1 = 2U_2$		$H_1 = H_2, U_2 = 0$		$M_1 = 2, M_2 = 1$	
M_c	$M_c \cos\theta$	M_c	$M_c \cos\theta$	M_c	$M_c \cos\theta$
0.6	0.587	0.854	0.571	0.610	0.599
0.8	0.585	1.122	0.623	0.773	0.601
1.0	0.588	1.311	0.734	0.888	0.628
1.2	0.582			0.973	0.651
1.4	0.581			1.045	0.699
1.6	0.586			1.107	0.769

same trends were found for each case, indicating that these compressibility effects are fairly general. The boundary-layer solution is required only when a comparison of growth rates with experiments is sought. In each case, the curves split into two regimes. For $M_c < 0.6$ the two-dimensional wave is always the most amplified wave whereas, for $M_c > 0.6$, a three-dimensional wave of increasing obliquity is most amplified. The angle of the most amplified disturbance roughly corresponds to

$$M_c \cos\theta \approx 0.6 \quad (10)$$

Thus, the Mach number resolved across the disturbance wave is always in the vicinity of 0.6. This might be considered similar to the case of swept-back airfoils, where the key Mach number is $M_\infty \cos\theta$. Table 2 shows values of $M_c \cos\theta$ for spatially developing mixing layers constructed in three different ways, all using the boundary-layer mean flow, for comparison with experiments. The value is consistently 0.58–0.59 for case 1, $T_2/T_1 = 1.0$ and $U_2/U_1 = 0.5$, but shows some deviation at high Mach number for case 2, equal stagnation enthalpies $H_1 = H_2$ and $U_2/U_1 = 0.0$, and case 3, fixed $M_1 = 2.0$ and $M_2 = 1.0$.

Convective Mach Number

The convective Mach number was proposed by Bogdanoff³ and by Papamoschou and Roshko² as a parameter that collapses the available data for growth of compressible mixing layers. From linear theory, the variation of the amplification of the most unstable mode with convective Mach number is shown in Fig. 4 for the temporal stability of the time-developing mixing layer. The curve of the most amplified two-dimensional wave is found by varying the wave number α , until a maximum is found, keeping θ fixed at 0 deg. The curve for oblique waves is found by varying both wave number and angle until a maximum is obtained. Above $M = 0.6$, the three-dimensional waves are the most amplified and the curve of the most amplified oblique disturbance is a much better fit to the existing experimental data, as compiled in Papamoschou and

Roshko,² than the two-dimensional curve. Computations similar to those presented in Fig. 4 were performed for convective Mach numbers up to 3.2 and showed that, at least for the case of equal densities, the growth rate continues to decrease as Mach number is increased.

To check the convective Mach number concept and to provide data for comparison with experiment, curves of spatial amplification against convective Mach number were calculated. In each case, the compressible boundary-layer equations were solved for the mean flow, and most amplified disturbances (as a function of both frequency and angle) were computed. Figure 5 shows peak amplification plotted against Mach number, using three different methods of varying the convective Mach number:

1) Equal temperatures $T_2/T_1 = 1.0$ and fixed velocity ratio $U_2/U_1 = 0.5$.

2) Equal stagnation enthalpies $H_2/H_1 = 1.0$ and fixed velocity ratio $U_2/U_1 = 0.0$, corresponding to early experiments on the compressible mixing layer.

3) Fixed Mach numbers $M_1 = 2.0$ and $M_2 = 1.0$, with convective Mach number varied by changing the ratio of stagnation enthalpies and the velocity ratio.

A good collapse of the data with M_c is obtained for $M_c < 0.8$, but there is some divergence at high convective Mach numbers. Recent experimental data presented by Papamoschou²⁰ suggest that the actual convective velocity of large-scale structures in the mixing layer may not be well predicted by the convective Mach number approach, Eq. (2). The convective Mach number, being just the ratio of freestream velocity difference to the sum of the sound speeds,²⁰ may be simply a first-order compressibility parameter. Thus, the lack of collapse shown on Fig. 5 at high Mach numbers may be due to second-order compressibility effects, which cannot be correlated by such a simple parameter.

Direct Numerical Simulations

In this section, results from direct simulations of the compressible Navier-Stokes equations are used to show the physics of vorticity transport behind the reduction in mixing-layer growth rate as Mach number is increased. The linear eigenfunctions are also investigated to see whether the same vorticity transport mechanisms are at work in the linearized problem.

Methods and Results

A two-dimensional code was used for these simulations, since it is the reduction in growth rate of the two-dimensional instability of the mixing layer that is initially responsible for the lower growth rate (i.e., up to $M_c = 0.6$). Simulations are performed for the time-developing mixing layer, which is periodic in the streamwise direction (x), allowing the use of

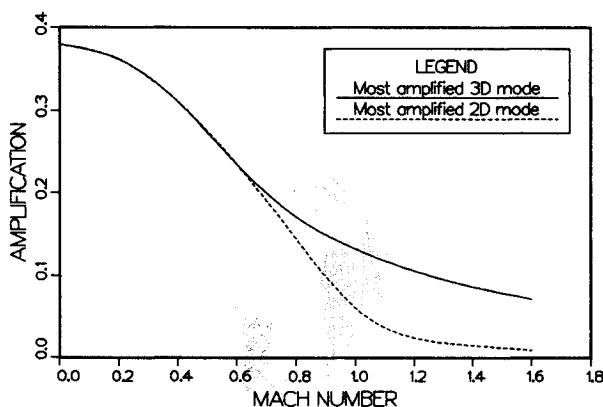


Fig. 4 Growth rate against Mach number showing the most amplified two- and three-dimensional disturbances.

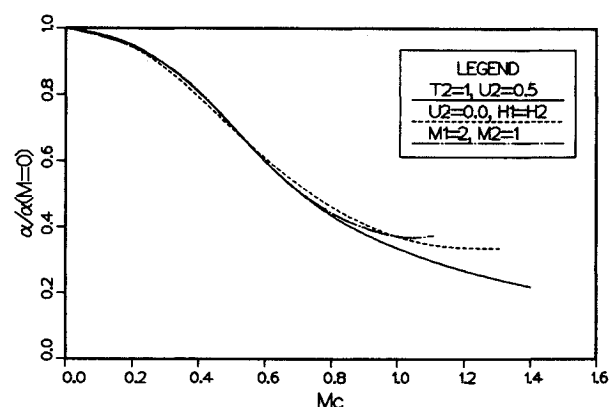


Fig. 5 Convective Mach number check. Plots show the most amplified mode in each case.

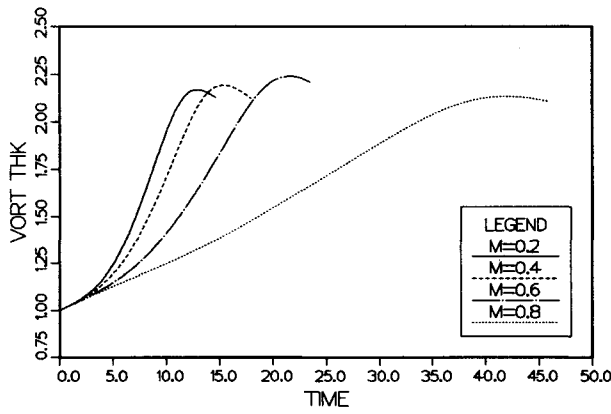


Fig. 6 Effect of Mach number on the growth of vorticity thickness.

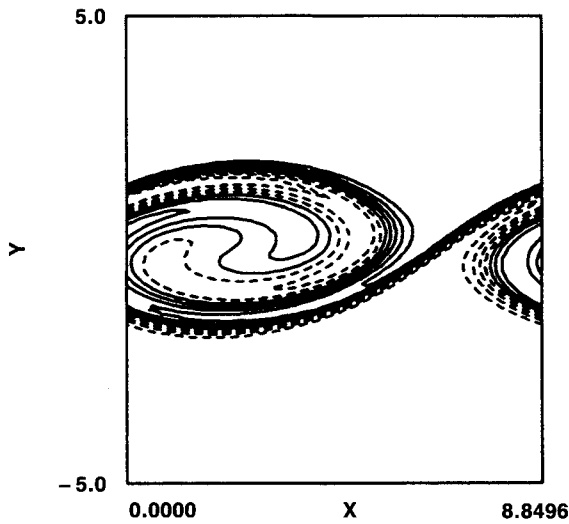


Fig. 7 Mixture fraction calculated from direct simulation at $M_c = 0.6$.

Fourier differentiation. In the y direction, we used a high-order modified Padé scheme developed by Lele,^{21,22} with characteristic/nonreflecting boundary conditions of the form proposed by Thompson²³ applied away from the shear layer to simulate an infinite domain in the y direction. Time advance was by a third-order Runge-Kutta scheme. More details of the simulation methods are given in Sandham and Reynolds.¹³ The computations were performed for the nonlinear growth of the fundamental instability mode. A hyperbolic tangent mean velocity profile was used, with temperature obtained from the Crocco-Busemann relation. The perturbation eigenfunctions were superimposed on the mean profile, with a relative amplitude of 5%, where the eigenfunctions were initially normalized by the magnitude of the largest eigenfunction \hat{u} . The simulations were made with $N_x \times N_y = 64 \times 81$, at a Reynolds number based on initial vorticity thickness and freestream velocity of 400, which was sufficiently low to resolve the flow fully.

A plot of vorticity thickness against time is shown on Fig. 6, for Mach numbers 0.2, 0.4, 0.6, and 0.8. The growth rate of the most amplified disturbance in the flow is clearly damped with increasing Mach number. Above $M_c = 0.7$, the flow develops shock waves^{13,21,22} embedded around the large-scale vortical structures. The supersonic modes of instability, which are the only two-dimensional unstable modes in the mixing layer at high Mach number, develop very slowly and radiate into the freestream, relative to which they are supersonic, forming a pattern of shock waves and expansion fans.¹³ How-

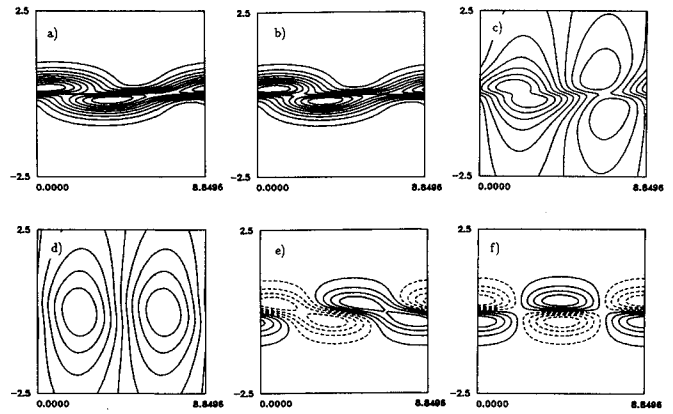


Fig. 8 Results from direct simulation at $M_c = 0.6$: a) ω ; b) ω/ρ ; c) ρ ; d) pressure; e) $-\text{vorticity} \times \text{dilatation}$; f) baroclinic term.

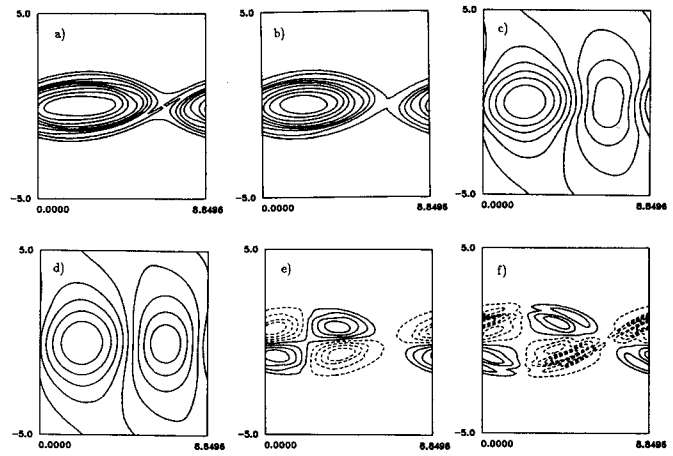


Fig. 9 Eigenfunctions from linear theory at $M_c = 0.6$: a) ω ; b) ω/ρ ; c) ρ ; d) pressure; e) $-\text{vorticity} \times \text{dilatation}$; f) baroclinic term.

ever, the fact that three-dimensional waves are amplified more than two-dimensional waves above $M_c = 0.6$ suggests that three-dimensional simulations need to be considered at the higher Mach numbers.²⁴ A passive scalar was computed along with the four flow variables, and a plot of a mixture fraction from the simulation at $M_c = 0.6$ is shown on Fig. 7. Other details of the developed structure are shown in Fig. 8.

Comparison with Linear Eigenfunctions

In this section, we consider the physics underlying the reduction in growth rate of the spanwise structure and the extent to which this is contained within the linear stability theory.

The compressible vorticity equation can be written in the following forms:

$$\omega_z = \frac{\partial u}{\partial y} - \frac{\partial v}{\partial x} \quad (11)$$

$$\frac{D\omega_z}{Dt} = -\omega_z \left(\frac{\partial u}{\partial x} + \frac{\partial v}{\partial y} \right) + \frac{1}{\rho^2} \left(\frac{\partial p}{\partial x} \frac{\partial \rho}{\partial y} - \frac{\partial p}{\partial y} \frac{\partial \rho}{\partial x} \right) \quad (12)$$

$$\frac{D(\omega_z/\rho)}{Dt} = \frac{1}{\rho^3} \left(\frac{\partial p}{\partial x} \frac{\partial \rho}{\partial y} - \frac{\partial p}{\partial y} \frac{\partial \rho}{\partial x} \right) \quad (13)$$

Selected terms from these equations are plotted on Fig. 8, for the direct simulation of a single vortex at $M = 0.6$. It was found that a change in the structure of the mixing layer occurs at high Mach numbers due to the dilatational and baroclinic

terms on the right-hand side of the preceding equations. In particular, the vortex becomes elongated in the streamwise direction (Fig. 8a) because both these terms are negative, and hence reduce vorticity, ahead of the vortex and are positive behind the vortex. It was found that the dilatational term on the right-hand side of Eq. (12) was stronger than the baroclinic term by a factor of 3 or 4, so that the change in structure is more apparent in the plots of ω than ω/ρ . The new elongated structure cannot entrain as much fluid as the original near-circular structure, and hence the growth rate of the mixing layer is reduced. The structure of the density and pressure fields is shown in Figs. 8c and 8d. Pressure and density are both lowered in the vortex cores and increased in the braid region between vortices. The assumption of an isentropic process from the freestream to the stagnation point in the braid was found to give a good prediction of fluid properties at that point.

Similar information can be found from the linear results by generating contour plots of the eigenfunctions at time $t = 0$. For example, the real part of the u velocity

$$u = \bar{u} + a \Re [\bar{u} e^{i\alpha x}] \quad (14)$$

can be found over one wavelength in the x direction and, similarly, derivatives of the flow variables can be easily found. Results are shown in Figs. 9a–9f for various flow quantities at $M = 0.6$. The amplitude of the disturbance, a , was chosen to be 0.5 for the spanwise vorticity ω_z , as well as for ω_z/ρ and ρ , to better illustrate the structure, which would otherwise be dominated by the mean flow. The remaining plots use a disturbance amplitude of 0.01. It should be noted that the y coordinate in these figures has been stretched by a factor of 2 to show the details more clearly.

Even at $M = 0.6$ the plots of ω_z and ω_z/ρ are little different from the vorticity structure for the incompressible case, found by Michalke.¹⁴ The two “elementary vortices” in the eigen-solution will subsequently grow to sufficient amplitude to become nonlinear and then rotate around each other and merge to form the fundamental vortex in the mixing layer. What is interesting is that the density and pressure disturbance fields (Figs. 9c and 9d) show striking similarities to the fields presented in Figs. 8c and 8d from the nonlinear roll-ups in the mixing layer. Low density and pressure perturbations are found in the vortex core, and high density and pressure are found in the region between vortices where the braid will eventually form.

The terms on the right-hand side of the compressible vorticity equations are plotted on Figs. 9e and 9f. Both the baroclinic and dilatational terms are negative (dashed contours) in precisely those regions where the elementary vortices develop. Thus, the most amplified two-dimensional disturbance in the compressible mixing layer tends to resist further growth since the right-hand side of the vorticity transport equation is removing vorticity from the location where vortex roll-up is trying to occur. Clearly, the growth rate of the disturbance is reduced by the effects of compressibility.

The appearance of the same physical processes in the linear eigensolutions that are observed in the later nonlinear development, as found by direct numerical simulation, may help to explain the surprising finding that the linear amplification is directly linked to mixing-layer growth rate.

Conclusions

It has been shown that the linear theory can be a very useful tool for investigating the compressible mixing layer. In particular:

1) The maximum amplification found from spatial theory, using the solution of the compressible boundary-layer equations as the mean flow, appears to be directly proportional to the growth rate of the developed mixing layer. This was demonstrated for the effect of density and velocity ratios on

mixing-layer growth rate at low Mach number.

2) Oblique waves are dominant in the mixing layer above a convective Mach number of 0.6. The obliquity of the most amplified wave selected by the linear theory is such that the convective Mach number resolved across the wave is approximately 0.6. We therefore expect that, above a convective Mach number of 0.6, the mixing layer will have a strongly three-dimensional structure. Further investigation of this topic can be found in Sandham and Reynolds.²⁴ The lack of collapse observed in the linear amplifications for three different methods of achieving high convective Mach numbers suggests that the convective Mach number may just be a first-order compressibility parameter.

3) Strong baroclinic and dilatational effects were observed to change the shape of the vortices that develop in the compressible mixing layer, producing structures elongated in the streamwise direction. The eigensolutions of the linear theory provide important details about the physics of the initial instability, which later develops into the large-scale structures. In particular, the reduction in growth rate of the two-dimensional instability can be explained by considering the terms in the linearized vorticity equations, using data from the linear eigensolutions.

Acknowledgments

This work has been sponsored by the U.S. Air Force Office of Scientific Research. Computing facilities were provided by the NASA-Ames Research Center. Also, Sanjiva Lele provided many helpful ideas.

References

- Brown, G. L. and Roshko, A., “On Density Effects and Large Structure in Turbulent Mixing Layers,” *Journal of Fluid Mechanics*, Vol. 64, Pt. 4, 1974, pp. 775–816.
- Papmoschou, D. and Roshko, A., “The Compressible Turbulent Shear Layer: An Experimental Study,” *Journal of Fluid Mechanics*, Vol. 197, 1988, pp. 453–477.
- Bogdanoff, D. W., “Compressibility Effects in Turbulent Shear Layers,” *AIAA Journal*, Vol. 21, June 1983, pp. 926–927.
- Gropengieser, H., “Study on the Stability of Boundary Layers and Compressible Fluids,” NASA TT F-12,786, Feb. 1970.
- Lessen, M., Fox, J. A., and Zien, H. M., “Stability of the Laminar Mixing of Two Parallel Streams with Respect to Supersonic Disturbances,” *Journal of Fluid Mechanics*, Vol. 25, 1966, pp. 737–742.
- Blumen, W., Drazin, P. G., and Billings, D. F., “Shear Layer Instability of an Inviscid Compressible Fluid. Part 2,” *Journal of Fluid Mechanics*, Vol. 71, 1975, pp. 305–316.
- Ragab, S. A. and Wu, J. L., “Instabilities in the Free Shear Layer Formed by Two Supersonic Streams,” AIAA Paper 88-0038, Jan. 1988.
- Zhuang, M., Kubota, T., and Dimotakis, P. E., “On the Instability of Inviscid, Compressible Free Shear Layers,” AIAA Paper 88-3538, 1988.
- Monkewitz, P. A. and Huerre, P., “Influence of the Velocity Ratio on the Spatial Instability of Mixing Layers,” *Physics of Fluids*, Vol. 25, 1982, pp. 1137–1143.
- Morkovin, M. V., “Guide to Experiments on Instability and Laminar-Turbulent Transition in Shear Layers,” NASA-Ames short course, 1988.
- Huerre, P. and Monkewitz, P. A., “Absolute and Convective Instabilities in Free Shear Layers,” *Journal of Fluid Mechanics*, Vol. 159, 1985, pp. 151–168.
- White, F. M., *Viscous Fluid Flow*, McGraw-Hill, New York, 1974, p. 195.
- Sandham, N. D., and Reynolds, W. C., “A Numerical Investigation of the Compressible Mixing Layer,” Mechanical Engineering Department, Stanford Univ., Stanford, CA, Rept. TF-45.
- Michalke, A., “On the Inviscid Instability of the Hyperbolic Tangent Velocity Profile,” *Journal of Fluid Mechanics*, Vol. 19, 1965, pp. 543–546.
- Lowery, P. S. and Reynolds, W. C., “Numerical Simulation of a Spatially-developing, Forced, Plane Mixing Layer,” Report TF-26, Mechanical Engineering Department, Stanford Univ., Stanford, CA, 1986.

¹⁶Bogdanoff, D. W., "Interferometric Measurement of Heterogeneous Shear-Layer Spreading Rates," *AIAA Journal*, Vol. 22, Nov. 1984, pp. 1550-1555.

¹⁷Dimotakis, P. E., "Two-Dimensional Shear-Layer Entrainment," *AIAA Journal*, Vol. 24, Nov. 1986, pp. 1791-1796.

¹⁸Fiedler, H. E., "Transport of Heat Across a Plane Turbulent Mixing Layer," *Advances in Geophysics*, Vol. 18A, Academic, 1974, pp. 93-109.

¹⁹Dimotakis, P. E. and Brown, G. L., "The Mixing Layer at High Reynolds Number: Large-Structure Dynamics and Entrainment," *Journal of Fluid Mechanics*, Vol. 78, 1976, pp. 535-560.

²⁰Papamoschou, D., "Structure of the Compressible Turbulent

Shear Layer," AIAA Paper 89-0126, Jan. 1989.

²¹Lele, S., "Vortex Evolution in Compressible Free Shear Layers," Workshop on the Physics of Compressible Turbulent Mixing, Princeton, NJ, Oct. 1988.

²²Lele, S., "Direct Numerical Simulation of Compressible Free Shear Flows," AIAA Paper 89-0374, Jan. 1989.

²³Thompson, K. W., "Time Dependent Boundary Conditions for Hyperbolic Systems," *Journal of Computational Physics*, Vol. 68, 1987, pp. 1-24.

²⁴Sandham, N. D. and Reynolds, W. C., "Growth of Oblique Waves in the Mixing Layer at High Mach Number," Preprint for *Turbulent Shear Flows 7*, Stanford Univ., Stanford, CA, Aug. 1989.

*Recommended Reading from the AIAA
Progress in Astronautics and Aeronautics Series . . .*



Dynamics of Explosions and Dynamics of Reactive Systems, I and II

J. R. Bowen, J. C. Leyer, and R. I. Soloukhin, editors

Companion volumes, *Dynamics of Explosions* and *Dynamics of Reactive Systems, I and II*, cover new findings in the gasdynamics of flows associated with exothermic processing—the essential feature of detonation waves—and other, associated phenomena.

Dynamics of Explosions (volume 106) primarily concerns the interrelationship between the rate processes of energy deposition in a compressible medium and the concurrent nonsteady flow as it typically occurs in explosion phenomena. *Dynamics of Reactive Systems* (Volume 105, parts I and II) spans a broader area, encompassing the processes coupling the dynamics of fluid flow and molecular transformations in reactive media, occurring in any combustion system. The two volumes, in addition to embracing the usual topics of explosions, detonations, shock phenomena, and reactive flow, treat gasdynamic aspects of nonsteady flow in combustion, and the effects of turbulence and diagnostic techniques used to study combustion phenomena.

Dynamics of Explosions
1986 664 pp. illus., Hardback
ISBN 0-930403-15-0
AIAA Members \$49.95
Nonmembers \$84.95
Order Number V-106

Dynamics of Reactive Systems I and II
1986 900 pp. (2 vols.), illus. Hardback
ISBN 0-930403-14-2
AIAA Members \$79.95
Nonmembers \$125.00
Order Number V-105

TO ORDER: Write, Phone, or FAX: AIAA c/o TASC0,
9 Jay Gould Ct., P.O. Box 753, Waldorf, MD 20604
Phone (301) 645-5643, Dept. 415 ■ FAX (301) 843-0159

Sales Tax: CA residents, 7%; DC, 6%. Add \$4.75 for shipping and handling of 1 to 4 books (Call for rates on higher quantities). Orders under \$50.00 must be prepaid. Foreign orders must be prepaid. Please allow 4 weeks for delivery. Prices are subject to change without notice. Returns will be accepted within 15 days.